Lead (Pb) Deposition onto New and Biofilm-laden Potable Water Pipes

Md Haddiuzaman[1], Nahreen Mirza[2], Shawn P Brown[2], David A Ladner[3], Maryam Salehi[4*]

[1] *Department of Civil Engineering, The University of Memphis, Memphis, TN, USA*
[2] *Department of Biological Sciences, The University of Memphis, Memphis, TN, USA*
[3] *Department of Environmental Engineering and Earth Sciences, Clemson University, Anderson, SC, USA*
[4] *Department of Civil and Environmental Engineering, University of Missouri, Columbia, MO, USA*

msalehiesf@gmail.com, mshfp@missouri.edu

Lead (Pb) Deposition onto New and Biofilm-laden Potable Water Pipes

Abstract

Heavy metals' interactions with plumbing materials are complicated due to the differential formation of biofilms within pipes that can modulate, transform, and/or sequester heavy metals. This research aims to elucidate the mechanistic role of biofilm presence on Lead (Pb) accumulation onto crosslinked polyethylene (PEX-A), high-density polyethylene (HDPE), and copper potable water pipes. For this purpose, biofilms were grown on new pipes for three months. Five-day Pb exposure experiments were conducted to examine the kinetics of Pb accumulation onto the new and biofilm-laden pipes. Additionally, the influence of Pb initial concentration on the rate of its accumulation onto the pipes was examined. The results revealed greater biofilm biomass on the PEX-A pipes compared to the copper and HDPE pipes. More negative zeta potential was found for the biofilm-laden plastic pipes compared to the new plastic pipes. After five days of Pb exposure under stagnant conditions, the biofilm-laden PEX-A (980 µg m^{-2}) and HDPE (1,170 µg m^{-2}) pipe accumulated more than three times the Pb surface loading compared to the new PEX-A (265 µg m^{-2}) and HDPE pipes (329 µg m^{-2}), respectively. However, under flow conditions, Pb accumulation on biofilm-laden plastic pipes was lower than on the new pipes. Moreover, with increasing the initial Pb concentration, greater rates of Pb surface accumulation were found for the biofilm-laden pipes compared to the new pipes under stagnant conditions. First-order kinetics models best described the Pb accumulation onto both new and biofilm-laden water pipes under both stagnant and flow conditions.

Key Words: Tap water quality, Plastic pipes, Lead, Biofilm, Heavy metals, Zeta potential

1. Introduction

Drinking water quality can deteriorate substantially within building plumbing systems. The surface area to volume ratio of water pipes within buildings is significantly greater than that of water distribution systems, allowing greater physicochemical and microbiological interactions between the pipe wall and bulk water (Zlatanović et al., 2017). With the rapid movement toward sustainability, plastic pipes are increasingly being used to rehabilitate aging water infrastructure and construct new potable water systems, which reduces cost and ameliorates drinking water quality concerns associated with metal pipe corrosion. Plastic potable water pipes are corrosion-resistant and recyclable. Moreover, they have a lightweight, long service life and low carbon footprint (Hajibabaei et al., 2018). The global demand for plastic pipes has been estimated to grow by more than 4% per annum (Stewart, 2005). Cross-linked polyethylene (PEX) plumbing has emerged as a common material with

prevalent applications starting in the mid to late 1990s (Tech Topic: PEX, 2012; Currence, 2017). HDPE pipes initially replaced stormwater culverts in the 1980s and have been utilized for water supply pipes (Currence, 2017). Although plastic potable water pipes are significant alternatives to metallic pipes, the interactions between these pipes with microbial and heavy metal contaminants in the water remained largely unexplored. Research is needed to better understand the drivers of contaminant fate and transfer within these materials to ensure safe drinking water for consumers.

Lead (Pb) in tap water remains a serious ongoing threat to public health (DeSimone et al., 2020; Yang & Faust, 2019). Lead exposure can result in severe acute and chronic health impacts, such as irreversible developmental and behavioral delays in children (Jain et al., 2005; Edwards et al., 2009; Deshommes et al., 2016; Salehi et al., 2017; Rísová, 2019). Lead in tap water predominantly originates from the corrosion of lead-bearing plumbing materials, including lead service lines, brass valves and fittings, galvanized iron, lead-tin solder, and faucets (Boyd et al., 2008; Ghoochani et al, 2021). Lead service lines, which are frequently found in older buildings, can be connected to the recently renovated building plastic plumbing systems. Thus, service line corrosion products can be released into the building plumbing and subsequently accumulate on the inner surface of plastic pipes (Maas et al., 2007). Moreover, the brass fittings used for connecting the PEX plumbing materials could release heavy metals into the tap water. In our published field study, we quantified lead concentrations at cold and hot water fixtures during the first three months after installation of the new PEX plumbing. Even though new plastic plumbing was used, we found a greater level of lead inside the building than in the water collected from the service line (Salehi et al., 2018).

Despite the assumption by water utilities and regulatory agencies about the inert nature of plastic plumbing materials, our recent bench-scale experiments and field study demonstrated that plastic surfaces act as resting sites for heavy metals (Salehi et al., 2017; Salehi et al., 2018). Our recent studies (Huang et al., 2020; Salehi, 2022) and the findings of others (Wingender & Flemming, 2004; Huang et al., 2017; Huang et al., 2019) showed that plastic pipes accumulate metal coatings in addition to biofilms on their surface after years of use. We demonstrated that the aged PEX-A (387 µg m^{-2}) and HDPE (418 µg m^{-2}) pipes deposited significantly greater levels of Pb compared to the new PEX-A (288 µg m^{-2}) and HDPE (335 µg m^{-2}) pipes after 5 d of exposure to Pb aqueous solution of 300 µg L^{-1} under stagnant conditions (Huang et al., 2020). The research conducted by Huang et al. (2019) revealed that Pb was released by upstream brass and metal pipes onto the downstream PEX plumbing (Huang et al., 2019). Plastic pipe surfaces are generally exposed to Pb concentrations above the US Environmental Protection Agency (USEPA) action level (> 15 µg L^{-1}). This exposure could be under stagnant water conditions, elevated temperatures, or pressurized conditions that might impact adsorption (Triantafyllidou & Edwards, 2012). Systematic research is needed to identify how heavy

metal uptake by plastic pipes differs from pellets, which have been studied extensively (Holmes et al., 2012, 2014; Huang et al., 2020), to better understand their fate in the built environment.

Biofilms are layers of amalgams of microorganisms and associated extracellular components that adhere to the surface of the pipe that is in direct contact with water (Kerr et al., 1998). They can interact with and influence metal ion sequestration within plumbing materials (Kerr et al., 1998; Costerton et al., 1987; Critchley et al., 2001). Although drinking water is disinfected prior to distribution, the disinfectant decay allows the survival of many microorganisms and their subsequent regrowth on the pipe's inner walls as biofilms. A recent study by Wang et al. (2022) revealed that plasticizers (e.g., phthalate ester) released by plastic potable water pipes into contact water promoted biofilm formation (Wang et al., 2022). Despite several studies conducted on biofilm accumulation on plastic potable water pipes in comparison to copper pipes, limited attention has been paid to the interaction of the biofilms present on the plastic pipe with heavy metals [e.g., Pb, Cu, Zn] that could be present in tap water. Our recent study revealed that the lead accumulated new and biofilm-laden plastic and copper potable water pipes could release their deposited lead as they were exposed to lower pH water under stagnant and flow conditions (Ghoochani et al., 2023).

Interactions between biofilms and scale may facilitate the continued development of both pipe surfaces. Reports suggest that water chemistry influences biofilm growth on plastic plumbing materials (Ji et al., 2015; Douterelo et al., 2016). While research has been conducted on the interactive effects of biofilms on pipe corrosion (Burleigh et al., 2014; Vargas et al., 2014; Rhoads et al., 2017; Marsili et al., 2018), the mechanistic role of biofilms present on plastic pipe surface on heavy metal sequestration has been overlooked. As our recent studies have revealed, the fundamental processes that control metal interactions with water infrastructure plastics remain poorly understood (Ahamed et al., 2020; Huang et al., 2020; Salehi, 2022). Thus, this research aims to elucidate the influence of biofilm presence on Pb deposition onto the PEX-A and HDPE potable water pipes compared to the copper pipes under water flow and stagnant conditions.

2. Experimental

2.1 Materials

Cross-linked polyethylene (PEX-A), high-density polyethylene (HDPE), and copper pipes were used in this study. The inner diameter of the PEX-A, HDPE, and copper pipes was 1.7 cm, 2.1 cm, and 1.91 cm, respectively. The pipes were purchased from a local hardware store (Memphis, TN, USA). Inductively coupled plasma mass spectrometry (ICP-MS) lead (Pb) (1000 mg L^{-1} in 3% nitric acid) standard solution was purchased from RICCA chemical company (Arlington, TX, USA). Clorox disinfectant comprised of 7.5% sodium hypochlorite (NaOCl) was purchased from a local store (Memphis, TN, USA). Nitric acid (70% purity) was purchased from Fisher Scientific (Hanover Park,

IL, USA). All the experiments were performed using ultrapure Milli-Q™ (18MΩ*cm) treated water unless it is described otherwise.

2.2 Pipe Disinfection and Biofilm Growth

The PEX-A and HDPE pipe loops were constructed using ten pipes, each with a length of 2.7 m (9 ft), while for the copper pipe loop, ten pipes, each with a length of 3.0 m (10 ft) were used. Copper and PEX-A pipes were connected using brass connectors, while HDPE pipes were connected using polyvinyl chloride (PVC) connectors. After constructing the separate pipe loops, the pipes were shock disinfected, in which the pipe loops were filled with chlorinated municipal tap water (20 ± 1 mg L^{-1} as Cl_2) for 40 min. After that, each of the pipe loops was flushed with tap water for 30 min. Then, the pipe rigs were connected to the municipal tap water supply for biofilm development (**Figure SI-1a**). The municipal tap water was groundwater chlorinated for primary and secondary disinfection processes, aerated, and filtered. The corrosion inhibitor was orthophosphate (1 mg L^{-1}). Tap water ran through the pipe loops at 2.0 ± 0.2 L min^{-1} for a daily cycle of 16 h of flow and 8 h of stagnation at room temperature to emulate standard household usage. Tap water quality parameters were measured weekly, including temperature, pH, dissolved oxygen (DO), and total chlorine concentrations. After biofilm generation for 90 d, pipes were removed from the stand and sectioned into 30 cm segments to undergo metal exposure experiments. In addition, representative pipe sections were used for microbial biomass and zeta potential measurements. Biofilm characterization was conducted using a droplet digital PCR system as described in **SI-1**.

2.3 Zeta Potential Measurement

Zeta potential measurements were conducted using an electrokinetic analyzer (SurPASS, 2010 model, Anton Paar USA, Ashland, VA) for new and biofilm-laden PEX-A and HDPE pipes to identify how the plastic pipe surface charge varies due to the biofilm accumulation. More information about mounting the samples and adjustment for analysis is described in **SI-2**. An automated titration was performed. After measuring the zeta potential at the original solution pH (usually between 5.5 and 6), small (~0.1 mL) doses of 0.1 N HCl were added to the solution until the pH dropped by at least 0.3 pH units. The zeta potential was measured four times (two in one flow direction and two in the reverse flow direction) at each pH point. This continued until the solution pH was near 3. The solution was then replaced by 500 mL of fresh KCl (0.1 mM), and a similar titration was performed but with 0.1 N NaOH until the pH was near 9. Total titration and measurement time were between 3 and 4 h. Data from the two runs were combined, and a titration curve of zeta potential versus pH between 3 and 9 was generated.

2.4 Lead (Pb) Exposure Experiments and Kinetics Modeling

The synthetic tap water was used for the experiments to ensure that the chemical composition of the water used for the metal exposure experiments was consistent (Ahamed et al., 2020; Hadiuzzaman et al., 2023). A comparison of the chemical composition of the synthetic tap water and municipal water used for the biofilm growth process is shown in **Table SI-1**. The 5 d kinetics experiments were conducted in triplicate through six-time intervals (2, 6, 12, 24, 48, and 120 h) (Hadiuzzaman et al., 2022) under stagnant and flow conditions with initial Pb concentration of 300 µg L^{-1}. To study the influence of initial Pb concentration on its accumulation onto the new and biofilm-laden water pipes, the pipe sections were exposed to five different aqueous solutions with Pb concentrations of 50, 150, 500, 750, and 1000 µg L^{-1} at pH=7.8 for 48 h. For the kinetics experiments that were conducted under flow conditions, 5.0 mL samples were collected from the water tank at different time intervals (2, 6, 12, 24, 48, and 120 h). However, for studying the influence of Pb initial concentration, 5.0 mL samples were collected after 48 h. Additional information about Pb exposure experiments and control samples is provided in **SI-3**. Information regarding the water quality measurements and lead quantifications is provided in **SI-4**. The statistical analyses conducted to compare the Pb accumulation results are described in **SI-5**. The kinetics of Pb adsorption onto the new and biofilm-laden PEX-A, HDPE, and copper pipes were investigated through first-order and second-order reaction kinetics models where the equilibrium Pb surface loading was calculated by averaging the Pb surface loadings during the last two exposure periods (48 h and 120 h).

3. Results And Discussions

3.1 Biomass Accumulation onto the Pipe Surfaces

The biomass accumulation onto the inner pipe surfaces after three months of biofilm growth was studied through the quantification of 16S ribosomal RNA genes (rDNA) using triplicates. The results revealed the greatest (p-value < 0.05) initial biofilm formations were on PEX-A pipes ($2.97 \times 10^9 \pm 3.24 \times 10^8$ copies cm^{-2}, mean ± standard deviation) compared to HDPE ($1.19 \times 10^8 \pm 2.03 \times 10^8$ copies cm^{-2}) and copper pipes ($1.07 \times 10^8 \pm 9.29 \times 10^7$ copies cm^{-2}). The biofilm biomass was not statistically different among copper and HDPE pipes (p-value > 0.05). It is uncertain at this time if the communities that make up these biofilms are similar across this pipe material or if they are distinct, which may indicate differential microbial-mediated adsorption potential. Organics leached by plastic pipes [e.g., antioxidants, stabilizers, monomers] can further support the growth of microorganisms on the pipe surface (Salehi, et al., 2018; Salehi et al., 2020). The finding of a smaller extent of biofilm formation on the copper pipes versus the PEX-A pipes agrees with the other published studies that reported this result due to the antibacterial properties of the copper pipes (Inkinen et al., 2018). On the other hand, the organics leached by plastic pipes are reported that they promote microbial regrowth (Inkinen et al., 2018). PEX-A pipes are known to significantly contribute to the assimilable

organic carbon (AOC) release that could promote microbial regrowth within the pipes (Connell et al., 2016). The study conducted by Connell et al. (2016) revealed a greater rate of AOC release from PEX pipes compared to the HDPE pipes after 7 d exposure to the water (Connell et al., 2016). The quantification of dissolved organic carbon (DOC) release into the contact water from new HDPE and PEX-A pipes showed that 1.1 ± 0.3 mg L^{-1} and 1.9 ± 0.1 mg L^{-1} of DOC were leached into the contact water after 120 h of stagnation. The lower organics released by HDPE pipes compared to the PEX-A pipes could be the reason for a lower microbial growth on these pipes. Moreover, it should be noted that biofilm growth onto the PEX-A pipes was conducted from April to July, and biofilm growth onto the HDPE pipes was conducted from May to August. However, water flow and room temperature were constant during the biofilm growth process for all three types of pipes. The average temperature, total chlorine residuals, and DO concentration during the biofilm growth were recorded as 21.2 ± 1.2 °C, 0.9 ± 0.1 mg L^{-1}, and 9.3 ± 0.2 mg L^{-1} for PEX-A pipes, 22.7 ± 1.2 °C, 1.0 ± 0.1 mg L^{-1}, and 9.1 ± 0.2 mg L^{-1} for HDPE pipes, and 21.6 ± 1.3 °C, 0.95 ± 0.1 mg L^{-1}, and 9.3 ± 0.1 mg L^{-1} for copper pipes. Moreover, the microbial content and the physiochemical characteristics [e.g., temperature] of the water that entered the pipe loops might be slightly different and, consequently, may have influenced the extent of biomass accumulated onto each type of pipe.

3.2 Surface Charge Variations Due to the Biofilm Accumulation

Studying the zeta potential is the key parameter to understand how electrostatic attractions of lead species toward the pipe surface vary by biofilm presence. The literature indicated that the negative charge associated with the bacterial cells could promote electrostatic attractions of heavy metal ions present within the contact water and thus enhance their uptake (Wasserman et al., 2000). In this study, zeta potential measurements were conducted for new and biofilm-laden PEX-A and HDPE pipes to obtain a better insight into the pipes' surface chemistry, which influences their interactions with the charged Pb species present in the aqueous solution. As inferred from **Figure 1**, all new and biofilm-laden pipes demonstrated a negative surface charge at neutral pH. The extracellular polymer substances (EPS), lipoteichoic and lipopolysaccharide components present in biofilm tend to make more negative surface charge (Harper et al., 2019). The magnitude of zeta potential is reduced with increasing the pH. This finding corroborates those found by Chu et al. (2019) reported a negative zeta potential for microplastics (Chu et al., 2019). The zeta potential of both new and biofilm-laden pipes showed a similar descending trend with increasing the pH, with biofilm-laden PEX-A and HDPE pipes being slightly more negative than the new PEX-A and HDPE pipes. At low pH values, the hydrophilic sites on the pipe surface have a great tendency to adsorb protons due to the elevated proton concentration, which results in less negative zeta potential; however, with increasing the pH, the pipe surface becomes more negatively charged, this process called deprotonation (Liu, 2021).

The zeta potential of new and biofilm-laden PEX-A varied from 55 to -97 mV and -24 to -120 when increasing the pH from 3 to 8.9. The zeta potential of new and biofilm-laden HDPE varies between 0 to -125 mV and -26 to -124 by increasing the pH from 3.1 to 8.6. The increased negativity of zeta potential for the biofilm-laden pipes suggests that biofilms may facilitate general increases in the magnitude of negative zeta potentials. Increasing the pipes' negative surface charge may result in increased Pb cation attachment. This result is similar to the literature that indicated increasing in the magnitude of negatively charged biofilms increases the likelihood of heavy metal sorption (Kurniawan & Fukuda, 2022). Our recent studies demonstrated the water pH variation in PEX-A potable water plumbing in a residential building to vary between 7.5 to 9.4 (Salehi et al., 2020). Considering this pH range, it could be inferred that new and biofilm-laden plastic pipes have negative surface charges. Additionally, the surface chemistry analysis of control samples that were prepared by removal of biofilm from the biofilm-laden plastic pipes showed no surface oxidation. Thus, it could be inferred that surface charge variation is solely due to biofilm growth (**Figure SI-2 and SI-3**).

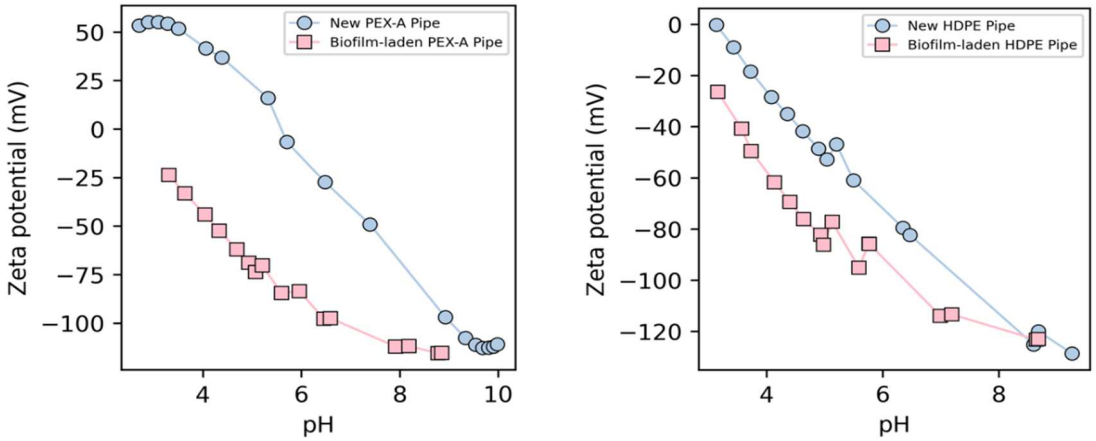

(a) (b)

Figure 1. The zeta potential variations versus pH for new and biofilm-laden (a) PEX-A and (b) HDPE water pipe

3.3 Lead Accumulation onto the New and Biofilm-laden Water Pipes Under Stagnant Condition

In this study, the Pb accumulations onto the new and biofilm-laden PEX-A, HDPE, and copper pipes under stagnant conditions and as a function of exposure duration were compared. As shown in **Figure 2**, during the entire exposure period, Pb accumulation onto the new copper pipes was significantly greater than both new PEX-A (p-value < 0.05) and new HDPE pipes (p-value < 0.05), and even biofilm-laden PEX-A (p-value < 0.05), and biofilm-laden HDPE pipes (p-value < 0.05). The equilibrium Pb surface loading on new copper pipes (1,391 µg m^{-2}) was more than 5 times greater than new PEX-A (265 µg m^{-2}) and 4 times greater than new HDPE pipes (329 µg m^{-2}). However, the

biofilm presence significantly increased the Pb accumulation onto the PEX-A (p-value < 0.05) and HDPE (p-value < 0.05) pipes compared to their new pipes during the 5 d metal exposure period under stagnant conditions (**Figure 2**). At equilibrium, the biofilm-laden PEX-A pipes have more than three times greater Pb loading (980 µg m^{-2}) compared to the new PEX-A pipes (265 µg m^{-2}). It should be noted that our control experiments that examined the Pb loading in biofilm-laden PEX-A pipes before the metal exposure process showed that Pb surface loading on biofilm-laden PEX-A pipes was 30.3 µg m^{-2}, whereas it was below the detection limit for the new pipes prior to the metal exposure experiment.

The biofilm-laden HDPE pipes accumulated approximately three times more Pb at equilibrium (1,170 µg m^{-2}) than the new HDPE pipes (329 µg m^{-2}). The biofilm-laden HDPE pipes accumulated 90% of its equilibrium Pb surface loading, while the new HDPE pipes obtained almost all their equilibrium Pb surface loadings during the first two hours of Pb exposure. The biofilm-laden HDPE pipes acquired 85% of $[Pb]_t$ in the synthetic tap water as their equilibrium surface loading after 5 d of metal exposure experiments; however, the new HDPE pipes only accumulated 24% of $[Pb]_t$ at equilibrium. It should be noted that our control experiments that examined the Pb loading in biofilm-laden HDPE pipes before the metal exposure process showed that Pb surface loading on biofilm-laden HDPE pipes was 44.3 µg m^{-2}, whereas it was below the detection limit for the new pipes prior to the metal exposure experiment. The 1 ft HDPE pipe segment was exposed to a greater volume of Pb aqueous solution (92 mL) compared to the 1 ft PEX-A pipe segment (65 mL) because of its larger diameter than PEX-A pipes. The initial Pb mass to surface area ratio for a PEX-A pipe segment was 1.2 mg m^{-2} however it was 1.4 mg m^{-2} for an HDPE pipe segment. Thus, a greater mass of Pb was available within the HDPE pipe system, which may have contributed to a greater Pb surface loading on both new and biofilm-laden HDPE pipes. Moreover, a different rate of organic leaching by plastic pipes may have influenced the Pb uptake behavior (Kelley et al., 2014; Salehi et al., 2020). The reduction of Pb surface loading on biofilm-laden HDPE pipes after 2 h of exposure, could be due to the release of initially accumulated Pb species that were loosely attached to the biofilm surface back into the water. However, an overall increasing rate of Pb accumulation for biofilm-laden HDPE pipes was found over the exposure duration of 5 d.

Despite the findings for PEX-A and HDPE pipes, the biofilm accumulation onto the copper pipes did not significantly increase the Pb accumulation under stagnant conditions. The biofilm-laden copper pipes (1,527 µg m^{-2}) accumulated more than the new copper pipe (1,352 µg m^{-2}), whereas the difference was not statistically significant (p-value > 0.05). At the equilibrium 93% of total Pb in the synthetic tap water was accumulated on the biofilm-laden copper pipe and 85% of total Pb was accumulated on new copper pipes. For copper pipes, biofilm surface accumulation is known to promote pipe corrosion and consequently release copper ions. Some of these released copper ions

could be stored within the biofilm structure, forming the complexation with the ligands that are already present within the extracellular polymeric substance of the biofilm (Galarce et al., 2020). The occupation of these available surface sites by Cu^{2+} ions likely reduce the available sites to accumulate Pb^{2+} species during the metal exposure experiments.

The ligands present within our synthetic tap water [OH^-, SO_4^{2-}, NO_3^-, Cl^-, HPO_4^{2-}, HCO_3^-, SiO_3^{2-}] could form both dissolved [e.g., Pb^{2+}, $Pb(OH)^+$] and insoluble Pb [e.g., $Pb(OH)_2$, $Pb_3(PO_4)_2$] complexes with Pb^{2+}. The Pb exposure experiments were conducted at the initial concentration of $[Pb]_t$=300 µg L^{-1} and pH=7.8. However, the aqueous system was closed, pH may have been changed as we conducted the metal exposure experiments. But we expect to have mostly Pb precipitates to be present in the system. The K_s values for $Pb(OH)_2$, $PbCO_3$, and $Pb_3(PO_4)_2$ are 4.2×10^{-15}, 1.5×10^{-13}, and 1.0×10^{-32} (SenGupta, 2017). So, $Pb_3(PO_4)_2$ controls the aqueous Pb concentration in this system. Thus, both adsorption and precipitation processes [accumulation] have occurred simultaneously in the studied aqueous system. As we reported earlier, the metal species adsorbed onto the plastic surface could act as nucleation sites to grow the precipitates. The low energy polymer sites, such as surface impurities, polymer terminal groups, or an arrangement of polymeric chains, could act as the nucleation sites for the precipitate formation (Salehi et al., 2017).

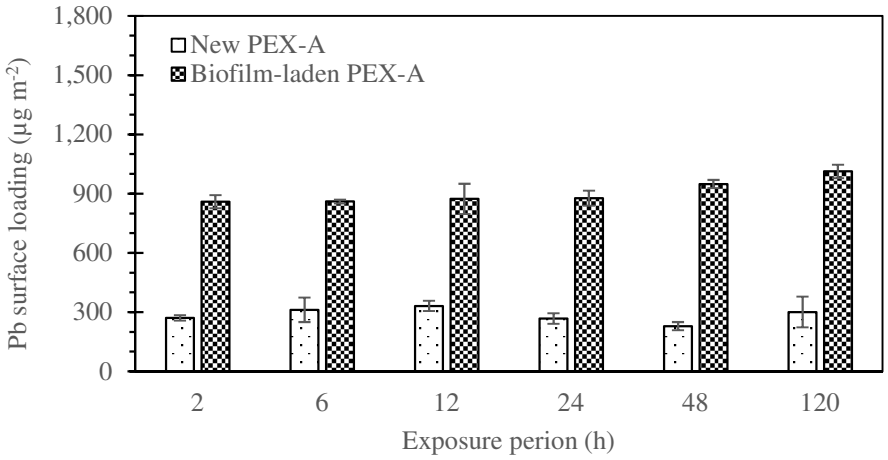

(a)

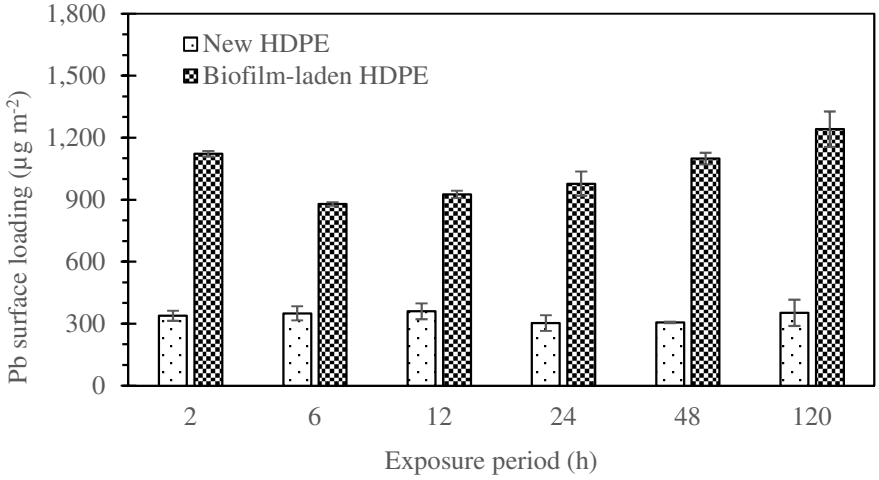

(b)

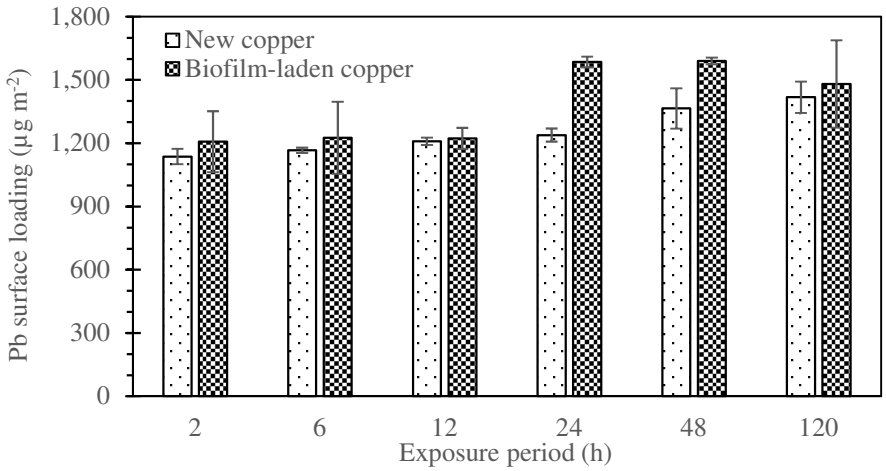

(c)

Figure 2. The results for Pb surface loadings on new and biofilm-laden (a) PEX-A (p-value < 0.05), (b) HDPE (p-value < 0.05), and (c) Copper (p-value > 0.05) water pipes over time, under stagnant condition

3.4 Lead Accumulation onto the New and Biofilm-laden Water Pipes Under Flow Condition

The Pb accumulation onto the plastic and copper water pipes under flow conditions was compared with the stagnant condition to better understand how variations of water use behavior within the residential and commercial buildings influence the extent of Pb accumulation onto the potable water pipes. Unlike our findings of increased Pb accumulation onto the plastic pipes due to the biofilm presence under stagnant conditions, we have found significant reductions (p-value < 0.05) in Pb surface loadings on both biofilm-laden PEX-A (p-value < 0.05) and HDPE (p-value < 0.05) pipes compared with their new pipes, under water flow conditions (**Figure 3**). This might be due to the shorter duration of Pb species interactions with the biofilm surface under flow conditions, which may not be sufficient to allow their removal from the aqueous system. The metal exposure experiments were conducted under consistent flow conditions to prevent the creation of the shear forces and

subsequent biofilm detachment. Although, it might be possible that some of the metal accumulated biofilms were released into the water due to their reduced internal cohesive strength caused by their aging or its nutrient starvation as exposed to the synthetic water and not the tap water (Boe-Hansen et al., 2002; Abe et al., 2012). **Table SI-1** demonstrates the differences in the chemical composition of synthetic tap water used for Pb exposure experiments and the municipal tap water that was used for the three months of the biofilm growth process.

Pb surface loading on the new copper pipes (15,918 µg m^{-2}) was not significantly different from on their biofilm-laden pipes (15,898 µg m^{-2}) (p-value > 0.05). The equilibrium Pb surface loadings onto the new and biofilm-laden PEX-A pipes were found as 18,300 µg m^{-2} and 18,219 µg m^{-2}, significantly greater (p-value < 0.05) than new (14,739 µg m^{-2}) and biofilm- laden HDPE (12,938 µg m^{-2}) pipes, respectively. Under flow conditions, a similar volume of 1 L was circulated in both PEX and HDPE pipe loops. Thus, available Pb mass was similar in both systems. However, a smaller surface area was exposed to the Pb aqueous solution in the PEX pipe segment (0.016 m^2) compared to the HDPE pipe segment (0.02 m^2). This might have contributed to the PEX-A pipes' greater Pb surface loading compared to the HDPE pipes under the flow conditions. Moreover, due to the greater volume of the Pb aqueous solution, the influence of organics leached by plastic pipes might be smaller compared to the stagnant condition. It should be mentioned that during our water flow experiments, a total of 1 L Pb aqueous solution of $[Pb]_t$=300 µg L^{-1} at pH=7.8 was circulated through the 30 cm pipe sections; however, in our stagnant experiments, the PEX-A, HDPE, and copper pipe sections were filled with 65 mL, 92 mL, and 100 mL of the Pb aqueous solution, respectively. Thus, the total mass of Pb (300 µg) present within the flow system was significantly greater than the Pb mass that was available under stagnant conditions. Therefore, it was expected to have a greater level of Pb accumulation onto all examined pipes under water flow conditions compared to the stagnant conditions.

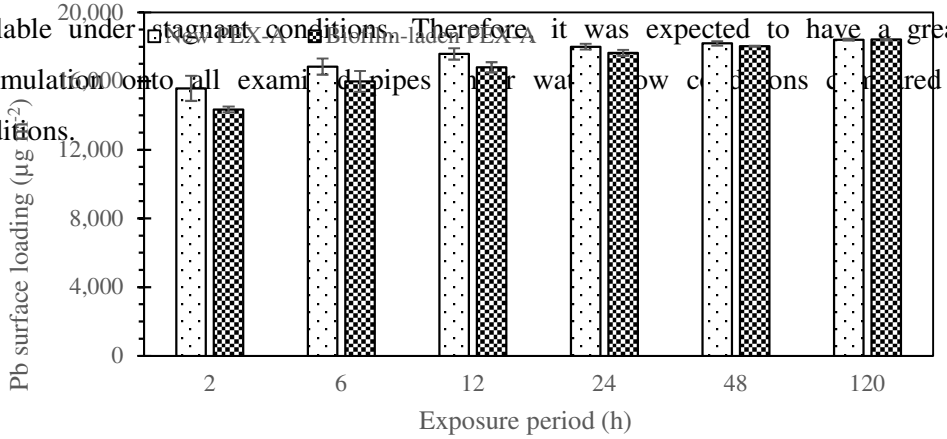

(a)

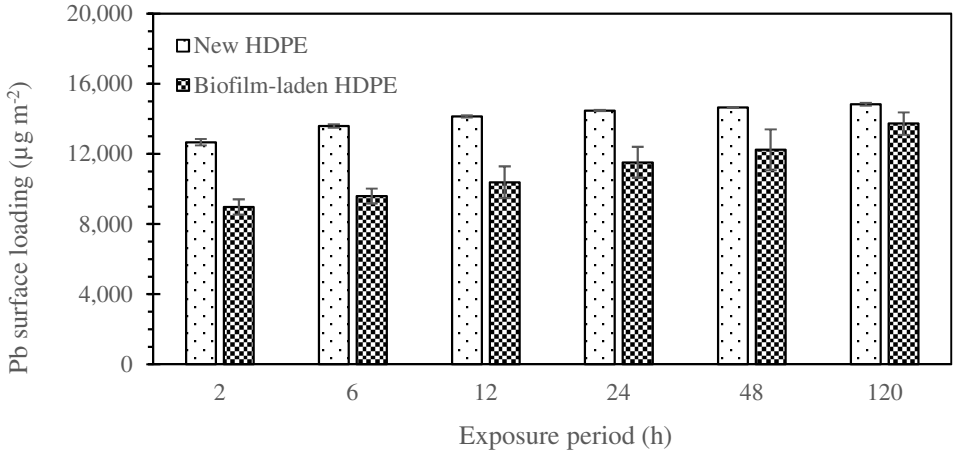

(b)

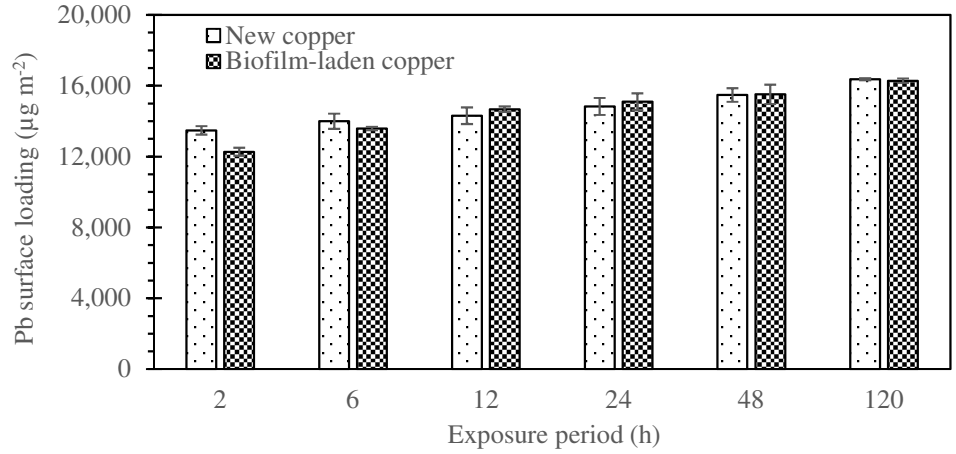

(c)

Figure 3. The results for Pb surface loadings on new and biofilm-laden (a) PEX-A (p-value < 0.05), (b) HDPE (p-value < 0.05) and (c) Copper (p-value > 0.05) water pipes over time under flow condition

3.5 The Kinetics Modeling for Lead Accumulation onto the New and Biofilm-Laden Water Pipes Under Stagnant and Flow Conditions

In this study, kinetics modeling was conducted to provide a better mechanistic understanding of the combined physiochemical mechanisms that control the rate of Pb accumulation onto the new and biofilm-laden potable plastic and copper water pipes. For this purpose, first-order and second-order reaction kinetics models were applied. The first-order kinetics model assumes that the rate of changes in the solute uptake over time is proportional to the difference in the saturation concentration and the amount of adsorbed solute over time (Romanov et al., 1998; Sahoo & Prelot, 2020). The first order reaction model mostly fits the experimental metal adsorption data when the solute adsorption proceeds through the diffusion to the solid micropores. However, the second-order reaction model assumes that the rate-limiting step is the chemisorption process (López-Luna et al., 2019; Sahoo &

Prelot, 2020). A non-linear chi-square (χ^2) comparison tests were conducted between the models (first and second order) to determine the best-fitted kinetics model for the studied pipes (**Table 1**).

The lower χ^2 values found here suggest that the first-order kinetics model better describes the Pb accumulation onto almost all water pipes tested. Thus, the diffusion of Pb species from the bulk aqueous phase to the pipe surface was likely the primary mechanism of Pb accumulation onto the pipe surface. This agrees with the Azizian (2004) theoretical study which demonstrated that at the high initial adsorbate concentration, the adsorption process of the kinetics studies can be described by the first-order reaction model, however, at low initial adsorbate concentration, it obeys the second-order reaction model (Azizian, 2004). The half-life ($t_{1/2}$) calculation revealed a longer duration half-life for biofilm-laden PEX-A (6.7 h) and HDPE (9.9 h) pipes compared to the new PEX-A (0.4 h) and HDPE (0.6 h) pipes. This finding suggests that Pb accumulation onto the new plastic pipes occurs more rapidly, as the most readily available surface deposition sites were rapidly occupied by the Pb species. However, despite the greater adsorption capacity of the biofilm-laden plastic pipes, they were not readily accessible for the Pb species, and consequently, a longer duration took to reach the half-life. It was completely different for the copper pipe as the half-life for new copper pipes (6.9 h) was greater than the half-life for the biofilm-laden copper pipe (1.8 h).

The kinetics data collected under water flow conditions also revealed that first-order reaction models best describe the Pb accumulation onto the new and biofilm-laden water pipes. This is clearly a mass transfer process due to the abundance of available Pb species in the system as water circulates through the pipes. The increased half-lives for the plastic pipes and decreased half-lives for the metal pipes due to the presence of biofilm were similar under both stagnant and flow conditions; however, the difference in half-lives between the new and biofilm-laden pipes under flow conditions was smaller than the one's under stagnant conditions. It can be due to the abundance of Pb species in the system as water circulated in the pipes. Moreover, this finding explains our results regarding the lower Pb accumulation onto the biofilm-laden plastic pipes compared to the new plastic pipes under flow conditions due to the short durations of Pb species contact with the biofilm that was not sufficient to allow a significant uptake of Pb species. Moreover, the convective diffusion in the flow conditions may have resulted in a faster mass transfer than pure diffusion occurred under stagnant conditions.

Table 1. The kinetics models' parameters and non-linear chi-square (χ^2) values for Pb accumulation onto the new and biofilm-laden water pipes under stagnant and flow conditions

Model / **Pipe**			**First-order reaction model**					**Second-order reaction model**		
Parameters			$q_{e,\ exp}$ ($\mu g\ m^{-2}$)	$q_{e,\ mod}$ ($\mu g\ m^{-2}$)	k_1 (h^{-1})	$t_{1/2}$, (h)	χ^2	$q_{e,\ mol}$ ($\mu g\ m^{-2}$)	$k_2 \times 10^3$ ($m^2 \mu g^{-1} h^{-1}$)	χ^2
Stagnant	New	Copper	1,391	1,416	0.101	6.9	0.42	1450	0.244	2.38
		PEX-A	265	288	1.890	0.4	1.87	285	90.0	1.48
		HDPE	329	335	1.200	0.6	0.12	356	3.0	2.12

	Biofilm-laden	Copper	1,535	1,553	0.381	1.8	0.18	1496	1.01	1.02
		PEX-A	981	1,011	0.104	6.7	0.91	1035	0.305	2.93
		HDPE	1,170	1,275	0.070	9.9	8.61	1286	0.183	10.49
Flow	New	Copper	15,917	16,380	0.090	7.7	13.08	16,769	0.02	43.21
		PEX-A	18,300	18,410	0.148	4.7	0.66	18,535	0.066	2.97
		HDPE	14,739	14,835	0.147	4.7	0.61	14,491	0.077	2.73
	Biofilm-laden	Copper	15,898	16,284	0.107	6.5	9.16	16,648	0.022	33.81
		PEX-A	18,219	18,412	0.122	5.7	2.03	18,643	0.036	9.65
		HDPE	12,938	13,734	0.073	9.6	41.03	14,501	0.01	158.80

3.6 Influence of Lead (Pb) Initial Concentration on the Rate of its Accumulation onto the Water Pipes

The influence of Pb initial concentration on the rate of its accumulation onto the new and biofilm-laden water pipes was investigated under stagnant (**Figure 4a**) and water flow conditions (**Figure 4b**). Under stagnant conditions, both new and biofilm-laden water pipes revealed a similar order of copper > PEX-A > HDPE for the increased rate of Pb surface accumulation by increasing the Pb initial concentration, and the accumulation onto the pipes was significantly different (p-value < 0.05). Under stagnant conditions, biofilm presence drastically increased the rate of Pb accumulation onto all water pipes with increasing the Pb concentration. A linearly increased Pb surface loading was found for new and biofilm-laden PEX-A and HDPE pipes ($R^2 \geq 0.90$) and copper pipes ($R^2 \geq 0.84$) with increasing the Pb concentration under stagnant conditions. By applying a linear model, the slopes are defined as the Pb accumulation rate at each condition. The Pb accumulation rate for new PEX-A, HDPE, and copper pipes under stagnant conditions varied from 0.004, 0.003, and 0.002 m to 0.099, 0.014, and 0.011 m due to the presence of biofilm.

Under stagnant condition, the greatest Pb surface loading onto the new PEX-A, HDPE, and copper pipes were found as 1,859, 1,472, and 2,536 µg m^{-2} and were significantly smaller than the maximum average Pb surface loadings onto the biofilm-laden PEX-A (3,162 µg m^{-2}), HDPE (3,094 µg m^{-2}), and copper pipes (5,240 µg m^{-2}), respectively. Under flow conditions, the Pb surface loading onto the new PEX-A, HDPE, and copper pipes increased linearly with raising the Pb concentration ($R^2 \geq 0.84$) (**Figure 4b**). Despite a similar trend, the coefficient of determination for this linear regression reduced when biofilm was present on the pipe surfaces ($R^2 \leq 0.74$) (**Figure 4b**). The greatest Pb surface loadings onto the new PEX-A, HDPE, and copper pipes under flow conditions varied from 58,427, 46,947, and 48,579 µg m^{-2} to 51,468, 29,185, and 41,288 µg m^{-2} due to biofilm presence. At almost all concentrations, less Pb surface loadings were found on the biofilm-laden water pipes compared to the new pipes under flow conditions.

The Pb accumulation rates onto the new PEX-A (120.49 m), HDPE (248.5 m), and copper pipes (0.688 m) reduced to the biofilm-laden PEX-A (0.397 m), HDPE (0.082 m), and copper pipes (0.234 m). As it was mentioned earlier, the short contact of the Pb species and biofilm surface during the water flow experiments may have resulted in insufficient interaction between those and, consequently, a lower accumulation rate compared to the new plastic pipes. Moreover, although the

calculation of the Reynolds number (Re < 1) for this system showed the laminar flow, some biofilm may have been detached from the pipe surface due to the alteration of water chemistry, biofilm maturation, and nutrient limitations. There was 18 h of flow and 6 h of stagnation during the biofilm growth process; however, the metal accumulation experiments for flow conditions were conducted for a continuous 48 h. Thus, this alteration of the water flow pattern may have contributed to the biofilm detachment; nutrient starvation and/or biofilm aging could reduce the biofilm matrix's internal cohesive strength and cause its detachment under lower shear stresses.

With increasing the Pb initial concentration, mostly Pb precipitates are present within the system. Thus, the surface sites available on both new and biofilm-laden water pipes act as the nucleation sites for the Pb precipitation and crystal growth as reported in our last study (Salehi et al., 2017). A similar trend of copper > PEX-A > HDPE was found for the Pb accumulation rates under stagnant conditions for both new and biofilm-laden water pipes. Thus, it could be inferred that copper provided more nucleation sites than both PEX-A and HDPE pipes. This finding is similar to the 5 d Pb exposure experiments, where the equilibrium Pb surface loading was greater for copper compared to the PEX-A and HDPE pipes. However, the Pb accumulation rates were not significantly different between PEX-A and HDPE pipes for both new and biofilm-laden pipes. Organics leached by plastic pipes may have made non-absorbable complexes with Pb and prevent their accumulation onto the pipe surface. Thus, a lower rate of Pb accumulation on plastic pipes was found compared to copper pipes. However, under the flow conditions, a greater volume of water (1 L) was in contact with the pipe segments thus, a lower concentration of the organics might be present within the system, which leads to forming of fewer complexes by Pb and consequently less prevention of its accumulation on the pipe surface. However, for both new and biofilm-laden water pipes, a greater rate of Pb accumulation was found for the PEX-A pipes compared to the HDPE pips; it could be due to the smaller surface area of the PEX-A pipe segment (0.016 m^2) that was exposed to 1 L of Pb aqueous solution compared to the HDPE pipe segment (0.020 m^2).

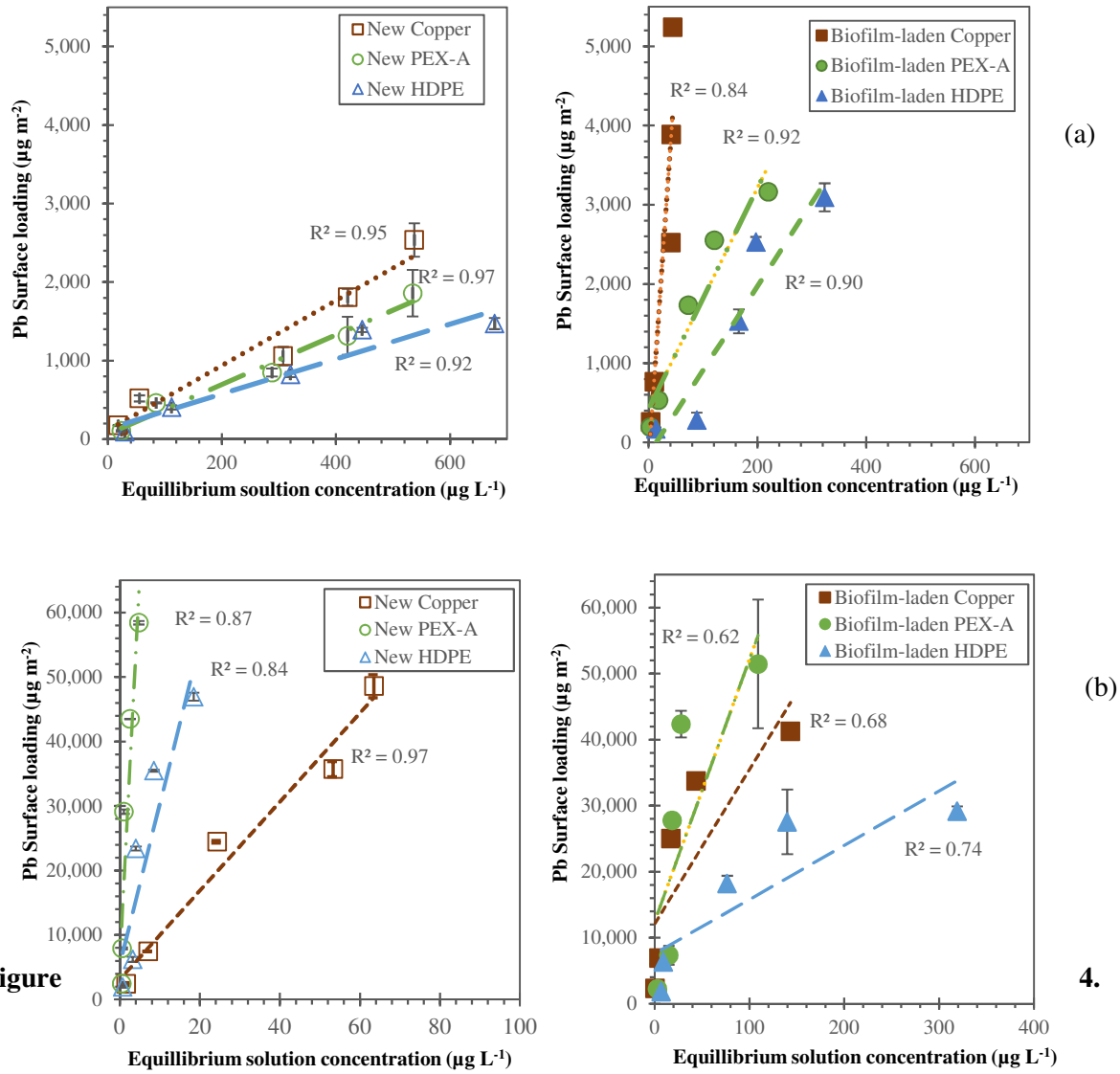

Figure 4. Equilibrium Pb surface loading for new and biofilm-laden PEX-A, HDPE, and copper pipes versus residual Pb in the contact water under (a) stagnant and (b) flow conditions

Although the biofilm (2.97×10^9 copies cm^{-2}) present onto the PEX-A pipes at the beginning of the Pb exposure period was an order of magnitude higher than HDPE pipes (1.19×10^8 copies cm^{-2}), biofilm accumulation onto both plastic pipes resulted in a significant increase in Pb surface loading. Biofilm accumulation onto the pipe surface could alter the metal accumulation behavior by facilitating the biosorption and transport of metals across cell walls, complexation, precipitation, and physical adsorption (Javanbakht et al., 2014). Moreover, as the zeta potential measurements revealed, biofilm formation on the pipe surface could make the surface charge more negative and promote the electrostatic attraction of the positively charged metal ions to the pipe surface.

Biofilm and heavy-metal interactions may occur through several potential mechanisms, including microbial-mediated biosorption (Chen et al., 2022; Su et al., 2023), metal-mediated alterations in microbial communities (Navarro-Noya et al., 2012; Caracciolo et al., 2021), metal-

mediated changes in biofilm gene expression (Portelinha & Angeles-Boza, 2021), and microbial-mediated metal transformations (Mohamed & Hatfield, 2005). Additional work is needed to identify the primary mechanism by which biofilms increase metal adsorption. Adsorption and sequestration of heavy metals into biofilms are facilitated by two major steps: 1) Metal ions undergo bulk diffusion into biofilm extracellular matrices, which is a complex amalgam of exopolysaccharides, proteins, fats, and free DNA that is heterogeneously and locally charged, and 2) Metal ions interact with solid surface and biofilm cellular walls. This interaction is complex and includes biosorption, bioaccumulation, resistance, and detoxification processes. Bioaccumulation occurs through metabolic activity between metals and living cells and may facilitate community turnover via local toxicity, favoring community members who can utilize or be minimally affected by these heavy metal species, which can lead to rapid turnover in biofilm communities when exposed to heavy metals (Ancion et al., 2010; Grün et al., 2018) **Figure SI-4** demonstrates the potential mechanisms of the heavy metal accumulation process onto the new and biofilm-laden plastic pipes (Galarce et al., 2020).

4. Conclusion

In this study, the mechanistic role of biofilm presence on the Pb accumulation onto the PEX-A, HDPE, and copper potable water pipes was investigated under stagnant and flow conditions. The biofilm presence on the plastic pipes' inner walls promoted the negative surface charge and provided more available surface sites for Pb accumulation under stagnant conditions; however, biofilm presence on the copper pipes did not enhance the Pb uptake, which might be due to its saturation with the Cu^{2+} ions. The water flow conditions significantly influenced the extent of Pb accumulation onto the new and biofilm-laden water pipes. Although biofilm presence significantly increased the Pb accumulation onto the PEX-A and HDPE pipes, it did not alter the Pb accumulation onto the copper pipes, under stagnant conditions. Under flow conditions, Pb accumulation onto both biofilm-laden PEX-A and HDPE pipes was reduced compared to their new pipes, which might be due to the shorter interactions of Pb species with the biofilm surface. Under stagnant conditions, biofilm presence on the pipe surface enhanced the Pb accumulation by possibly facilitating the biosorption and transport of metals across cell walls, complexation, precipitation, and physical adsorption. This study will provide a foundation for continued exploration of heavy metal fate in water infrastructure and provide an understanding of metal adsorption and biofilm interactions. Additionally, understanding how biofilm affects the surface charge of the pipes could have broader implications beyond heavy metals, as it may influence the fate and transport of other contaminants, including organics and microbiological agents.

Acknowledgments

Funding for this work was provided by the National Science Foundation (NSF) grant CBET-2029764. The authors thank Barry Wymore, the research technician in the College of Engineering at the University of Memphis, for building the pipe rig. The authors also thank Shima Ghoochani, the

graduate research assistant, and Colton Kirby, Carla Meier, Lauren Nichole Mitchell, and Rhianna Cameron Munns undergraduate research assistants in the Civil Engineering Department at the University of Memphis, for their assistance with conducting the metal exposure experiments. The authors would also like to thank Amy Abell and Nathan Mullins in the Department of Biological Sciences at the University of Memphis for their assistance in conducting ddPCR-based biomass quantification, Lingyun Peng in Clemson University for assistance with surface charge analysis, and Dibya Datta from University of Missouri for conducting the organic leaching experiments.

References

Abe, Y., Skali-Lami, S., Block, J. C., & Francius, G. (2012). Cohesiveness and hydrodynamic properties of young drinking water biofilms. *Water Res*, *46*, 1155–1166. https://doi.org/10.1016/J.watres.2011.12.013

Aghilinasrollahabadi, K., Salehi, M., & Fujiwara, T. (2020). Investigate the influence of microplastics weathering on their heavy metals uptake in stormwater. *J Hazard Mater*, *408*, 124439. https://doi.org/10.1016/j.jhazmat.2020.124439

Ahamed, T., Brown, S. P., & Salehi, M. (2020). Investigate the role of biofilm and water chemistry on lead deposition onto and release from polyethylene: an implication for potable water pipes. *J Hazard Mater*, *400*, 123253. https://doi.org/10.1016/j.jhazmat.2020.123253

Ancion, P. Y., Lear, G., & Lewis, G. D. (2010). Three common metal contaminants of urban runoff (Zn, Cu & Pb) accumulate in freshwater biofilm and modify embedded bacterial communities. *Environ Pollut*, *158*, 2738–2745. https://doi.org/10.1016/j.envpol.2010.04.013

Azizian, S. (2004). Kinetic models of sorption: a theoretical analysis. *J Colloid Interf Sci*, *276*, 47–52. https://doi.org/10.1016/j.jcis.2004.03.048

Boe-Hansen, R., Albrechtsen, H. J., Arvin, E., & Jørgensen, C. (2002). Bulk water phase and biofilm growth in drinking water at low nutrient conditions. *Water Res*, *36*, 4477–4486. https://doi.org/10.1016/S0043-1354(02)00191-4

Boyd, G. R., Pierson, G. L., Kirmeyer, G. J., & English, R. J. (2008). Lead variability testing in Seattle Public Schools. *J Am Water Works Assoc*, *100*, 53–64. https://doi.org/10.1002/j.1551-8833.2008.tb08142.x

Burleigh, T. D., Gierke, C. G., Fredj, N., & Boston, P. J. (2014). Copper tube pitting in Santa Fe municipal water caused by microbial induced corrosion. *Materials*, *7*, 4321–4334. https://doi.org/10.3390/ma7064321

Caracciolo, A. B., Terenzi, V., Saccà, L., & Manici, L. M. (2021). Rhizosphere microbial communities and heavy metals. *Microorganisms 2021, 9, 1462*. https://doi.org/10.3390/microorganisms9071462

Chen, S. Y., Wu, J. Q., & Sung, S. (2022). Effects of sulfur dosage on continuous bioleaching of heavy metals from contaminated sediment. *J Hazard Mater*, *424*, 127257. https://doi.org/10.1016/j.jhazmat.2021.127257

515 Chu, X., Li, T., Li, Z., Yan, A., & Shen, C. (2019). Transport of microplastic particles in
516 saturated porous media. *Water 2019, 11, 2474*. https://doi.org/10.3390/w11122474

517 Connell, M., Stenson, A., Weinrich, L., Lechevallier, M., Boyd, S. L., Ghosal, R. R., Dey, R.,
518 & Whelton, A. J. (2016). PEX and pp water pipes: assimilable carbon, chemicals, and odors.
519 *J Am Water Works Assoc*, *108*, E192–E204. https://doi.org/10.5942/jawwa.2016.108.0016

520 Costerton, J. W., Cheng, K. J., Geesey, G. G., Ladd, T. I., Nickel, J. C., Dasgupta, M., &
521 Marrie, T. J. (1987). Bacterial biofilms in nature and disease. *Annu Rev Microbiol*, *41*, 435–
522 464. https://doi.org/10.1146/annurev.mi.41.100187.002251

523 Critchley, M. M., Cromar, N. J., McClure, N., & Fallowfield, H. J. (2001). Biofilms and
524 microbially influenced cuprosolvency in domestic copper plumbing systems. *J Appl*
525 *Microbiol*, *91*, 646–651. https://doi.org/10.1046/j.1365-2672.2001.01417.x

526 Currence, D. (2017, September 18). Evolution of HDPE. *Wastewater Digest*.
527 https://www.wwdmag.com/pipe-distribution/pipe/article/10936117/evolution-of-hdpe

528 Deshommes, E., Andrews, R. C., Gagnon, G., McCluskey, T., McIlwain, B., Doré, E., Nour,
529 S., & Prévost, M. (2016). Evaluation of exposure to lead from drinking water in large
530 buildings. *Water Res*, *99*, 46–55. https://doi.org/10.1016/j.watres.2016.04.050

531 Coppens M. O., Froment G. F., Diffusion and reaction in a fractal catalyst pore—II.
532 Diffusion and first-order reaction, *Chem Eng Sci*, 50, 1027-1039,
533 https://doi.org/10.1016/0009-2509(94)00479-B.

534 DeSimone, D., Sharafoddinzadeh, D., Salehi, M. (2020), Prediction of Children's blood lead
535 levels from exposure to lead in schools' drinking water – A case study in Tennessee, USA,
536 *Water*, 12, 1826. doi.org/10.3390/w12061826
537

538 Douterelo, I., Husband, S., Loza, V., & Boxall, J. (2016). Dynamics of biofilm regrowth in
539 drinking water distribution systems. *Appl Environ Microbiol*, *82*, 4155–4168.
540 https://doi.org/10.1128/AEM.00109-16

541 Edwards, M., Triantafyllidou, S., & Best, D. (2009). Elevated blood lead in young children
542 due to lead-contaminated drinking water: Washington, DC, 2001-2004. *Environ Sci Technol*,
543 *43*, 1618–1623. https://doi.org/doi:10.1021/es802789w

544 Galarce, C., Fischer, D., Díez, B., Vargas, I. T., & Pizarro, G. E. (2020). Dynamics of
545 biocorrosion in copper pipes under actual drinking water conditions. *Water, 12, 1036*.
546 https://doi.org/10.3390/W12041036

547 Ghoochani, S., Salehi, M., DeSimone, D., Salehi, M., Bhattacharjee, L., (2022). Evaluating
548 the resiliency of schools' potable water systems toward interruption caused by the COVID-19
549 pandemic", *Environ. Sci.: Water Res. and Technol.* 8, 1223-1235.
550 doi.org/10.1039/D2EW00149G

551 Ghoochani, S., Hadiuzzaman, M., Mirza, N., Brown, S.P., Salehi, M. (2023). Lead release
552 from plastic potable water pipes under various water chemistry and flow conditions,
553 implications for plumbing decontamination, *Environmental Pollution*, 2023, Accepted.

Grün, A. Y., App, C. B., Breidenbach, A., Meier, J., Metreveli, G., Schaumann, G. E., & Manz, W. (2018). Effects of low dose silver nanoparticle treatment on the structure and community composition of bacterial freshwater biofilms. *Plos One*, *13*, e0199132. https://doi.org/10.1371/journal.pone.0199132

Hadiuzzaman, M., Ladner, D. A., & Salehi, M. (2023). Impact of the surface aging of potable water plastic pipes on their lead deposition characteristics. *Environ. Sci.: Water Res. Technol.* https://doi.org/10.1039/d3ew00043e

Hadiuzzaman, M., Salehi, M., & Fujiwara, T. (2022). Plastic litter fate and contaminant transport within the urban environment, photodegradation, fragmentation, and heavy metal uptake from storm runoff. *Environ Res*, *212*, 113183. https://doi.org/10.1016/j.envres.2022.113183

Hajibabaei, M., Nazif, S., & Tavanaei Sereshgi, F. (2018). Life cycle assessment of pipes and piping process in drinking water distribution networks to reduce environmental impact. *Sustain Cities Soc*, *43*, 538–549. https://doi.org/10.1016/j.scs.2018.09.014

Harper, R. A., Carpenter, G. H., Proctor, G. B., Harvey, R. D., Gambogi, R. J., Geonnotti, A. R., Hider, R., & Jones, S. A. (2019). Diminishing biofilm resistance to antimicrobial nanomaterials through electrolyte screening of electrostatic interactions. *Colloids Surf B Biointerfaces*, *173*, 392–399. https://doi.org/10.1016/j.colsurfb.2018.09.018

Holmes, L. A., Turner, A., & Thompson, R. C. (2012). Adsorption of trace metals to plastic resin pellets in the marine environment. *Environ Pollut*, *160*, 42–48. https://doi.org/10.1016/j.envpol.2011.08.052

Holmes, L. A., Turner, A., & Thompson, R. C. (2014). Interactions between trace metals and plastic production pellets under estuarine conditions. *Mar Chem*, *167*, 25–32. https://doi.org/10.1016/j.marchem.2014.06.001

Huang, X., Pieper, K. J., Cooper, H. K., Diaz-Amaya, S., Zemlyanov, D. Y., & Whelton, A. J. (2019). Corrosion of upstream metal plumbing components impact downstream PEX pipe surface deposits and degradation. *Chemosphere*, *236*, 124329. https://doi.org/10.1016/j.chemosphere.2019.07.060

Huang, X., Zemlyanov, D. Y., Diaz-Amaya, S., Salehi, M., Stanciu, L., & Whelton, A. J. (2020). Competitive heavy metal adsorption onto new and aged polyethylene under various drinking water conditions. *J Hazard Mater*, *385*, 121585. https://doi.org/10.1016/j.jhazmat.2019.121585

Huang, X., Zhao, S., Abu-Omar, M., & Whelton, A. J. (2017). In-situ cleaning of heavy metal contaminated plastic water pipes using a biomass derived ligand. *J Environ Chem Eng*, *5*, 3622–3631. https://doi.org/10.1016/j.jece.2017.07.003

Inkinen, J., Jayaprakash, B., Ahonen, M., Pitkänen, T., Mäkinen, R., Pursiainen, A., Santo Domingo, J. W., Salonen, H., Elk, M., & Keinänen-Toivola, M. M. (2018). Bacterial community changes in copper and PEX drinking water pipeline biofilms under extra disinfection and magnetic water treatment. *J Appl Microbiol*, *124*, 611–624. https://doi.org/10.1111/JAM.13662

595 Jain, N. B., Laden, F., Guller, U., Shankar, A., Kasani, S., & Garshick, E. (2005). Relation
596 between blood lead levels and childhood anemia in India. *Am J Epidemiol*, *161*, 968–973.
597 https://doi.org/10.1093/aje/kwi126

598 Javanbakht, V., Alavi, S. A., & Zilouei, H. (2014). Mechanisms of heavy metal removal
599 using microorganisms as biosorbent. *Water Sci Technol*, *69*, 1775–1787.
600 https://doi.org/10.2166/wst.2013.718

601 Ji, P., Parks, J., Edwards, M. A., & Pruden, A. (2015). Impact of water chemistry, pipe
602 material and stagnation on the building plumbing microbiome. *PLoS ONE*, *10*, 1–23.
603 https://doi.org/10.1371/journal.pone.0141087

604 Kelley, K. M., Stenson, A. C., Dey, R., & Whelton, A. J. (2014). Release of drinking water
605 contaminants and odor impacts caused by green building cross-linked polyethylene (PEX)
606 plumbing systems. *Water Res*, *67*, 19–32. https://doi.org/10.1016/j.watres.2014.08.051

607 Kerr, C. J., Osborn, K. S., Robson, G. D., & Handley, P. S. (1998). The relationship between
608 pipe material and biofilm formation in a laboratory model system. *J Appl Microbiol*, *85*, 29S-
609 38S. https://doi.org/10.1111/J.1365-2672.1998.tb05280.x

610 Kurniawan, A., & Fukuda, Y. (2022). Analysis of the electric charge properties of biofilm for
611 the development of biofilm matrices as biosorbents for water pollutant. *Energy Ecol Environ*,
612 1–7. https://doi.org/10.1007/s40974-022-00253-6/figures/3

613 Liu, Q. (2021). Zeta potential measurements for surface modification of plastic substrates for
614 nanofluidic biosensors [Louisiana State University].
615 https://digitalcommons.lsu.edu/gradschool_theses

616 López-Luna, J., Ramírez-Montes, L. E., Martinez-Vargas, S., Martínez, A. I., Mijangos-
617 Ricardez, O. F., González-Chávez, M. del C. A., Carrillo-González, R., Solís-Domínguez, F.
618 A., Cuevas-Díaz, M. del C., & Vázquez-Hipólito, V. (2019). Linear and nonlinear kinetic and
619 isotherm adsorption models for arsenic removal by manganese ferrite nanoparticles. *SN Appl*
620 *Sci*, *1*, 1–19. https://doi.org/10.1007/s42452-019-0977-3/tables/7

621 Maas, R. P., Patch, S. C., Christian, A. M., & Coplan, M. J. (2007). Effects of fluoridation
622 and disinfection agent combinations on lead leaching from leaded-brass parts.
623 *Neurotoxicology*, *28*, 1023–1031. https://doi.org/10.1016/j.neuro.2007.06.006

624 Marsili, E., Kjelleberg, S., & Rice, S. A. (2018). Mixed community biofilms and microbially
625 influenced corrosion. *Microbiol Aust*, *39*, 152– 157. https://doi.org/10.1080/154281196

626 Mohamed, M. M., & Hatfield, K. (2005). Modeling microbial-mediated reduction in batch
627 reactors. *Chemosphere*, *59*, 1207–1217. https://doi.org/10.1016/J.chemosphere.2004.12.013

628 Navarro-Noya, Y. E., Hernández-Mendoza, E., Morales-Jiménez, J., Jan-Roblero, J.,
629 Martínez-Romero, E., & Hernández-Rodríguez, C. (2012). Isolation and characterization of
630 nitrogen fixing heterotrophic bacteria from the rhizosphere of pioneer plants growing on mine
631 tailings. *Appl Soil Ecol*, *62*, 52–60. https://doi.org/10.1016/j.apsoil.2012.07.011

632 Portelinha, J., & Angeles-Boza, A. M. (2021). The antimicrobial peptide gad-1 clears
633 pseudomonas aeruginosa biofilms under cystic fibrosis conditions. *ChemBioChem*, *22*, 1646–
634 1655. https://doi.org/10.1002/cbic.202000816

635 Rhoads, W. J., Pruden, A., & Edwards, M. A. (2017). Interactive effects of corrosion, copper,
636 and chloramines on legionella and mycobacteria in hot water plumbing. *Environ Sci Technol*,
637 *51*, 7065–7075. https://doi.org/10.1021/acs.est.6b05616

638 Rísová, V. (2019). The pathway of lead through the mother's body to the child. *Interdiscip*
639 *Toxicol*, *12*, 1. https://doi.org/10.2478/intox-2019-0001

640 Romanov, A. E., Pompe, W., Beltz, G. E., & Speck, J. S. (1998). An approach to threading
641 dislocation "reaction kinetics". *Appl Phys Lett*, *69*, 3342. https://doi.org/10.1063/1.117300

642 Sahoo, T. R., & Prelot, B. (2020). Adsorption processes for the removal of contaminants
643 from wastewater: the perspective role of nanomaterials and nanotechnology. Nanomaterials
644 for the detection and removal of wastewater pollutants, *Micro Nano Technol*, 161–222.
645 https://doi.org/10.1016/b978-0-12-818489-9.00007-4

646 Salehi, M. (2022). Global water shortage and potable water safety; Today's concern and
647 tomorrow's crisis. *Environ Int*, *158*, 106936. https://doi.org/10.1016/j.envint.2021.106936

648 Salehi, M., Abouali, M., Wang, M., Zhou, Z., Nejadhashemi, A. P., Mitchell, J., Caskey, S.,
649 & Whelton, A. J. (2018). Case study: Fixture water use and drinking water quality in a new
650 residential green building. *Chemosphere*, *195*, 80–89.
651 https://doi.org/10.1016/j.chemosphere.2017.11.070

652 Salehi, M., Jafvert, C. T., Howarter, J. A., & Whelton, A. J. (2018). Investigation of the
653 factors that influence lead accumulation onto polyethylene: Implication for potable water
654 plumbing pipes. *J Hazard Mater*, *347*, 242–251.
655 https://doi.org/10.1016/j.jhazmat.2017.12.066

656 Salehi, M., Li, X., & Whelton, A. J. (2017). Metal accumulation in representative plastic
657 drinking water plumbing systems. *J Am Water Works Assoc*, *109*, E479–E493.
658 https://doi.org/10.5942/jawwa.2017.109.0117

659 Salehi, M., Odimayomi, T., Ra, K., Ley, C., Julien, R., Nejadhashemi, A. P., Hernandez-
660 Suarez, J. S., Mitchell, J., Shah, A. D., & Whelton, A. (2020). An investigation of spatial and
661 temporal drinking water quality variation in green residential plumbing. *J Build Environ*, *169*,
662 106566. https://doi.org/10.1016/j.buildenv.2019.106566

663 SenGupta, A. K. (2017). Table of Solubility Product Constants at 25 °C. In *Ion Exchange in*
664 *Environmental Processes* (pp. 459–460). *John Wiley & Sons, Inc*.
665 https://doi.org/10.1002/9781119421252.app3

666 Stewart, B. R. (2005). Corrosion resistance, ease of installation stimulate demand for plastic
667 pipe. *Plastics Engineering*, *61*, 14–22.

668 Su, P., Zhu, F., Ding, L., Abd Elnabi, M. K., Elkaliny, N. E., Elyazied, M. M., Azab, S. H.,
669 Elkhalifa, S. A., Elmasry, S., Mouhamed, M. S., Shalamesh, E. M., Alhorieny, N. A., Abd
670 Elaty, A. E., Elgendy, I. M., Etman, A. E., Saad, K. E., Tsigkou, K., Ali, S. S., Kornaros, M.,
671 & A-G Mahmoud, Y. (2023). Toxicity of heavy metals and recent advances in their removal:
672 a review. *Toxics 2023, Vol. 11, page 580*, *11*, 580. https://doi.org/10.3390/toxics11070580

673 *Tech Topic: PEX*. (2012). BNP media. Retrieved from
674 https://www.pmmag.com/articles/102114-tech-topic-pex , accessed on Sep 5th 2023

675 Triantafyllidou, S., & Edwards, M. (2012). Lead (Pb) in tap water and in blood: implications
676 for lead exposure in the United States, *Environ Sci Technol*, *42*, 1297–1352.
677 https://doi.org/10.1080/10643389.2011.556556

678 Vargas, I. T., Alsina, M. A., Pavissich, J. P., Jeria, G. A., Pastén, P. A., Walczak, M., &
679 Pizarro, G. E. (2014). Multi-technique approach to assess the effects of microbial biofilms
680 involved in copper plumbing corrosion. *Bioelectrochemistry*, *97*, 15–22.
681 https://doi.org/10.1016/j.bioelechem.2013.11.005

682 Wang, H., Yu, P., Schwarz, C., Zhang, B., Huo, L., Shi, B., & Alvarez, P. J. J. (2022).
683 Phthalate esters released from plastics promote biofilm formation and chlorine resistance.
684 *Environ Sci Technol*, *56*, 1081–1090. https://doi.org/10.1021/acs.est.1c04857

685 Wasserman, E., Felmy, A. R., & Chilakapati, A. (2000). Non-equilibrium thermodynamic
686 simulation of metal uptake in the bacterial electrical double-layer. *Colloids Surf B*
687 *Biointerfaces*, *18*, 19–29. https://doi.org/10.1016/S0927-7765(99)00122-8

688 Wingender, J., & Flemming, H. C. (2004). Contamination potential of drinking water
689 distribution network biofilms. *Water Sci Technol*, *49*, 277–286.
690 https://doi.org/10.2166/WST.2004.0861

691 Yang, E., & Faust, K. M. (2019). Dynamic public perceptions of water infrastructure in us
692 shrinking cities: end-user trust in providers and views toward participatory processes. *J Water*
693 *Resour Plan Manag*, *145*, 1–13. https://doi.org/10.1061/(asce)wr.1943-5452.0001093

694 Zlatanović, L., van der Hoek, J. P., & Vreeburg, J. H. G. (2017). An experimental study on
695 the influence of water stagnation and temperature change on water quality in a full-scale
696 domestic drinking water system. *Water Res*, *123*, 761–772.
697 https://doi.org/10.1016/j.watres.2017.07.019

698

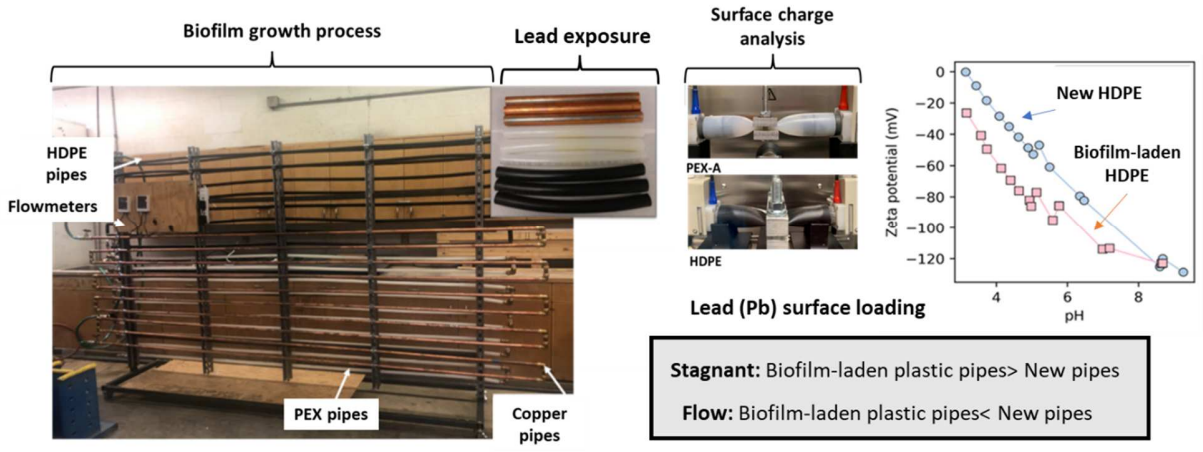

Stagnant: Biofilm-laden plastic pipes> New pipes

Flow: Biofilm-laden plastic pipes< New pipes